PROCEEDINGS OF SCIENCE

Multiplicity, Transverse Momentum, Forward-Backward Long Range Corrrelations and Percolation of strings

L.Cunqueiro, E.G.Ferreiro and C.Pajares*
Instituto Galego de Física de Altas Enerxías and Departamento de Física de Partículas, Universidade de Santiago de Compostela, 15782 Santiago de Compostela, Spain.
E-mail: pajares@fpaxp1.usc.es

The behaviour of the normalized variance of the multiplictiy distribution and the normalized transverse momentum fluctuations with centrality is naturally explained by the dependence on centrality of the number of clusters of color sources. This dependence predicts a nonmonotonic behaviour with centrality of the multiplicity associated to high p_T events. The clustering of color sources is also able to reproduce the increase with centrality of the forward-backward long-range correlations and its supression compared to superposition model predictions.

The 2nd edition of the International Workshop — Correlations and Fluctuations in Relativistic Nuclear Collisions —
July 7-9 2006
Galileo Galilei Institute, Florence, Italy

*Speaker.

PoS(CFRNC2006)019

1. Multiplicity and Transverse Momentum correlations

Event by event fluctuations of transverse momentum have been measured both at SPS and RHIC [1, 2, 3, 4, 5, 6, 7]. The data show a nontrivial behaviour as a function of the centralitly of the collision. Concretely, the nonstatistical normalized fluctuations grow as the centrality increases, with a maximum around $Npart \simeq 100-150$, followed by a decrease at larger centralities. The NA49 collaboration have presented their data on multiplicity fluctuations as a function of centrality for $Pb-Pb$ collisions [8, 9]. A nonmonotonic centrality (system size) dependence of the multiplicty scaled variance was found. Its behaviour is similar to the one obtained for the $\Phi(p_T)$ measure, used by the *NA*49 Collaboration to quantify the p_T fluctuations [2], suggesting that they are related to each other [11]. The Φ measure is independent of the distribution of the number of particle sources if the sources are identical and independent of each other. This implies that Φ would be independent of the impact parameter if the nucleus-nucleus collision was a simple superposition of nucleon-nucleon interactions.

In the framework of string clustering [12] such a behaviour is naturally explained [13, 14]. Let us remember the main features of the model. In a nucleus-nucleus collision, color strings are stretched between partons from the projectile and the target. This strings decay into new strings by $q-\overline{q}$ pair production and finally hadronize to produce the observed particles. For the decay of the strings we apply the Schwinger mechanism of fragmentation, where the decay is controlled by the string tension that depends on the color field of the string.

The strings have longitudinal and transverse dimensions, and the density of created strings in the first step of the collision depends on the energy and on the centrality of the collision. One can consider the number of strings N_S in the central rapidity region as proportional to the number of collisions, $N_A^{\frac{4}{3}}$, whereas in the forward and backward region it becomes proportional to the number of participants N_A. (We follow the dual parton model [15, 16] or the quark gluon string model [17]). We will use the variable

$$\eta = N_S \frac{S_1}{S_A} \tag{1.1}$$

proportional to the density of strings, where S_A corresponds to the nuclear overlap area, $S_A = \pi R_A^2$ for central collisions, and S_1, to the area of one string, $S_1 = \pi r_0^2$ ($r_0 \simeq 0.2-0.3$ fm). With the increase of energy and/or atomic number of the colliding nuclei, the density grows, so the strings begin to overlap forming clusters. We assume that a cluster of n strings that occupies an area S_n behaves as a single color source with a higher color field, generated by a higher color charge $\vec{Q}_n$. This charge corresponds to the vectorial sum of the color charge of each individual string $\vec{Q}_1$ The resulting color field covers the area S_n of the cluster. As $Q_n^2 = (\sum_{i=1}^n \vec{Q}_1)^2$ and since the individual string colors may be arbitrarily oriented, the average $\vec{Q}_{1i}\vec{Q}_{1j}$ is zero and therefore, $Q_n^2 = nQ_1^2$ if the strings fully overlap. Because the strings may overlap only partially we introduce a dependence on the area of the cluster,

$$Q_n = \sqrt{\frac{nS_n}{S_1}} Q_1. \tag{1.2}$$

Note that if the strings are just touching each other, $S_n = nS_1$ and $Q_n = nQ_1$, so the strings behave independently. On the contrary, if they fully overlap, $S_n = S_1$ and $Q_n = \sqrt{n}Q_1$. Knowing

Q_n, one can compute the multiplicity μ_n and the mean transverse momentum $< p_T >_n$ of the particles produced by a cluster of n strings [17, 18]. According to the Schwinger mechanism for the fragmentation of the clusters, one finds

$$< \mu >_n = \sqrt{\frac{nS_n}{S_1}} < \mu >_1, \;\; < p_T >_n = (\frac{nS_1}{S_n})^{\frac{1}{4}} < p_T >_1 \tag{1.3}$$

where $< \mu >_1$ and $< p_T >_1$ correspond to the mean multiplicity and the mean transverse momentum of the particles produced by one individual string. As the energy and/or the number of paricipants of the collision increase, the density of strings increases. At a certain critical density ($\eta_C \simeq 1.2 - 1.5$, depending on the nuclei-profile used) a macroscopical cluster appears wich marks the percolation phase transition, which is a second order, nonthermal phase transition. (The formation of a macroscopial cluster of strings can be seen as due to multiple partonic interactions, which can approximately give rise to a thermal spectrum. In this way, the critical percolation density is related to a critical temperature [18].)

To obtain the mean p_T and the mean multiplicity of the collision at a given centrality one needs to sum over all formed clusters and to average over all events

$$< \mu >= \frac{\sum_{i=1}^{N_{events}} \sum_j < \mu >_{nj}}{N_{events}}, \;\; < p_T >= \frac{\sum_{i=1}^{N_{events}} \sum_j < \mu >_{nj} < p_T >_{nj}}{\sum_{i=1}^{N_{events}} \sum_j < \mu >_{nj}}. \tag{1.4}$$

The sum over j goes over all individual clusters j, each one formed by n_j strings and occupying an area S_{nj}. The quantities n_j and S_{nj} are obtained for each event, using a Monte-Carlo code [16], based on the quark gluon string model. With our code, once we fix the energy and the nuclei of the collision, we obtain, for each event, a number of participant nucleons and a configuration for the created strings. Each string is generated at an identified impact parameter in the transverse space. Knowing the transverse area of each string, we identify all the clusters formed in each event, the number of strings n_j that conforms a cluster j and the area occupied by each cluster. We use a Monte-Carlo code for the cluster formation to compute the number of strings that come into each cluster and the area of the cluster. Conversely, we do not use a Monte-Carlo code for the decay of the cluster because we apply analytical expressions (eq. (1.4)). We assume that the multiplicity distribution of each cluster follows a Poissonian of mean value $< \mu >_{nj}$ and therefore the variance $< \mu^2 >_{nj} - < \mu >^2_{nj}$ is $< \mu >_{nj}$. It is easy to see that at low densities the scaled variance is given by

$$\frac{Var(\mu)}{< \mu >} = 1 + < \mu >_1$$

and at high densities,

$$\frac{Var(\mu)}{< \mu >} \longrightarrow 1.$$

Our results for the scaled variance for negative particles are presented in fig.(1). The rapidity interval is $4.0 < y < 5.5$. We have also included our results without cluster formation. One can observe that when clustering is included we find a good agreement with the experimental data. We see that the clustering produces a decrease of the scaled variance for central collisions, where the density of strings increases and the clustering has a bigger effect. At RHIC energies our results are

similar to the ones obtained at SPS energies. The fluctuations on the number of target participants at a fixed number of proyectile participants have been pointed out to be an important contribution to the scaled multiplicity variance [10, 19]. There are many string models which find no agreement with data because such fluctuations do not contribute to the projectile rapidity hemisphere (HIJING,URQMD,HSD). In these models, there is momentum exchange but no color exchange between partons of the projectile and the target. In DPM or QGSM there is color exchange and the strings connect both rapidity hemispheres. Although at very high density the scaled variance goes to one, our result is above one and also clearly above the experimental data. (The new NA49 data is clearly below one [10]). The reason for this difference is that we do not take into account the energy conservation in the formation of clusters due to the use of analytical formulae. In fact, in the forward rapidity range considered, at a large fixed number of projectile participants, the energy conservation implies that the number of strings and also the number of target participants are almost fixed in such a way that the scaled variance at high centrality is more supressed. This effect should be weaker at mid rapidity.

The PHENIX Collaboration [20] has measured the centrality dependence of the transverse momentum fluctuations using the observable F_{P_T} that quantifies the deviation of the observed fluctations from statistically independent particle emission:

$$F_{P_T} = \frac{\omega_{data} - \omega_{random}}{\omega_{random}} \tag{1.5}$$

where

$$\omega = \frac{\sqrt{< p_T >^2 - < p_T >^2}}{< p_T >}. \tag{1.6}$$

The comparison of our results for the dependence of F_{P_T} on the number of participants N_p to the PHENIX data is shown in fig.(2). An acceptable agreement is obtained.

The behaviour of the transverse momentum fluctuations as well as the behaviour of the multiplicity fluctuations can be understood as follows: at low density, most of the particles are produced by individual strings with the same $< p_T >$ and $< \mu >$, so the fluctuations are small. Similarly, at large density above the percolation critial point there is essentially only one cluster formed by most of the strings created in the collision and therefore fluctuations are not expected either.

In fig.(3) our results for the observable Φ_{P_T} of charged particles in Pb-Pb central collisions at 158AGeV are compared to the data of NA49 [2]. A good agreement is obtained.

PHENIX and STAR Collaborations have pointed out ([21, 22]) minijets as the main source of transverse momentum fluctuations. In our approach, these fluctuations have the same origin as the multiplicity fluctuations, namely the clustering of color sources. Since a cluster of strings produces particles with a harder p_T spectrum than in the unclustering case, our approach is compatible with the role of minijets in transverse momentum fluctuations at RHIC energies. Notice that at SPS energies there are transverse momentum fluctuations although the production of minijets is negligible. More studies on both p_T and Φ spaces would be very convenient, as it has been emphasized at this workshop [22].

Finally let us mention that our results are consistent with the clustering analysis[23] presented at this workshop.

2. Multiplicity associated to high p_T events and multiplicity fluctuations

The events which are self-shadowed have singular properties concerning the multiplicity distribution associated to them. We call self-shadowed events in hadron-hadron, hadron-nucleus or nucleus-nucleus collisions those events whose inelastic cross section depends only on the elementary cross section for such events [24]. Assuming that hadron-hadron, hadron-nucleus and nucleus-nucleus collisions are a superposition of independent elementary collisions, it is shown in [25] that the multiplicity distribution associated to self-shadowed events, $P_C(n)$ is approximately given in terms of the total multiplicity distribution $P(n)$ by

$$P_C(n) \simeq \frac{nP(n)}{< n >}. \tag{2.1}$$

There are many different self-shadowed events, for instance non-diffractive events, anihilation events in $\overline{p}A$ collisions, nonisolated fast baryons in pA or AA collisions, or high p_T events in hh, hA or AA collisions. Equation (2.1) has been checked in high energy pp collisions for the multiplicity distribution associated to W^{+-} and Z^0 production and also for the multiplicity distribution associated to jet production and annihilation [25]. In nucleus-nucleus collisions, data of ISR experiments [26] on events with $p_T \geq 3GeV$ produced in $\alpha - \alpha$ collisions also satisfy eq.(2.1).

The eq.(2.1) has been obtained assuming independent superposition of elementary interactions. This assumption is not justified for heavy nuclei collisions at RHIC energies where collective interactions, such as percolation of strings, are at work. However, it can be argued [27] that even in these cases, eq. (2.1) is approximately valid, considering the collision as a superposition of different clusters of elementary interactions (strings). Since high p_T events are self-shadowed, from eq. (2.1), we can write the difference between the average multiplicity associated to high p_T events $< n >_C$ and the total average multiplicity in terms of the scaled variance of the total multiplictiy distribution [27]:

$$< n >_C - < n >= \frac{< n^2 > - < n >^2}{< n >}. \tag{2.2}$$

The equation (2.1) can be easily checked experimetally.

3. Forward-Backward Long Range Correlations

In any model based on a superposition of elementary and statistically independent collisions, the squared forward-backward dispersion is proportional to the square dispersion of the number of elementary collisions [28]. In fact, we have

$$D^2_{FB} \equiv < n_F n_B > - < n_F >< n_B >=< N > (< n_{0F} n_{0B} > - < n_{0F} >< n_{0B} >) + (< N^2 > - < N >^2) < n_{0F} >< n_{0B} > \tag{3.1}$$

where N stands for the number of elementary interactions, $n_{0F}(n_{0B})$ for the number of forward(backward) produced particles in an elementary interaction and $n_F(n_B)$ for the total number of forward(backward) particles.

The first term of (3.1) is the correlation between particles produced in the same elementary interaction. Assuming these correlations to have short range in rapidity, this term vanishes if one takes a rapidty gap larger than $1-1.5$ units between the forward and backward rapidity intervals. In this way, one is left with the last term in (3.1). We see that there is a long range correlation between particles which are far away in rapidity. This correlation is due to the fluctation in the number of elementary interactions, controlled by unitarity. This term increases with the number of elementary interactions, therefore we expect that the long-range correlations increase with energy and the size of the nucleus in hh, hA and AA collisions. However, if there are interactions among strings, the number of independent elementary interactions translates approximately into the number of clusters of strings. Therefore a clear supression of long range correlations relative to the expected in a superposition picture is predicted [29, 30].

The preliminary data of STAR presented in this workshop [31] show that in fact there is a strong supression of long range correlations. In fig.(4) we compare the preliminary data, obtained with a rapidity gap of 1.6 units in the central rapidity region, and a forward and backward intervals of 0.2 units, to our results [32] of percolation of strings. A good agreements is obtained.

Finally, let us mention that the Color Glass Condensate (CGC) generates distintive predictions for the long-range component of the correlations [33]. The main contribution to this component is given by the diagram of fig.(5) which is

$$< \frac{dN_F}{dy_1}\frac{dN_B}{dy_2} >=< (\frac{dN}{dy})^2 > \sim \frac{\pi R^2 Q_S^2}{\alpha_S^2} \sim \frac{1}{\alpha_S}\frac{dN}{dy} \tag{3.2}$$

where Q_S is the saturation momentum.

On the contrary, the main contribution to the short range correlation is given by diagram of fig.(6). This diagram has two factors of α_S and should give a contribution to the total multiplicity fluctuations of order

$$< \frac{dN}{dy_1}\frac{dN}{dy2} > \sim \alpha_S \pi R^2 Q_S^4. \tag{3.3}$$

The different powers of α_S in eqs. (3.2) and (3.3) allow us to easily disentangle the long-range correlations from the short range correlations. The predictions of CGC are not very different from the percolation of strings ones, what is not unexpected given the similarities between both approaches.

We thank the organizers for such a nice meeting. This work was done under contract FPA2005-01963 of CICYT of SPAIN.

References

[1] H. Appelshauser *et al.* [NA49 Collaboration], Phys. Lett. B **459**, 679 (1999).

[2] T. Anticic *et al.* [NA49 Collaboration], Phys. Rev. C **70**, 034902 (2004).

[3] D. Adamova *et al.* [CERES Collaboration], Nucl. Phys. A **727**, 97 (2003).

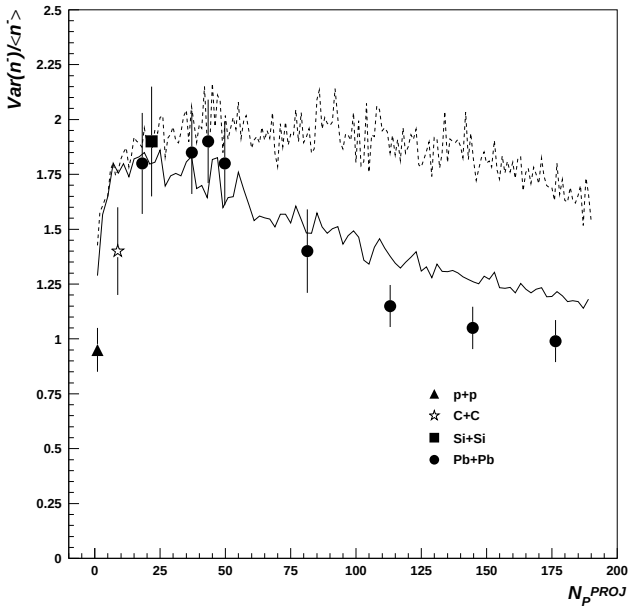

Figure 1: Our results for the scaled variance of negatively charged particles in Pb-Pb collisions at SPS energies compared to NA49 data. Solid line: clustering of colour sources. Dashed line: independent strings.

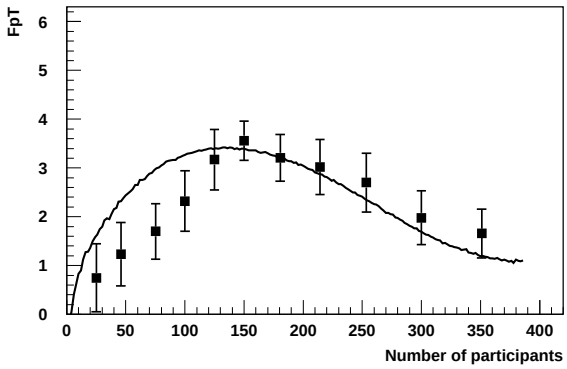

Figure 2: F_{P_T} versus the number of participants. Experimental data from PHENIX at $\sqrt{s} = 200GeV$ are compared to our results(solid line).

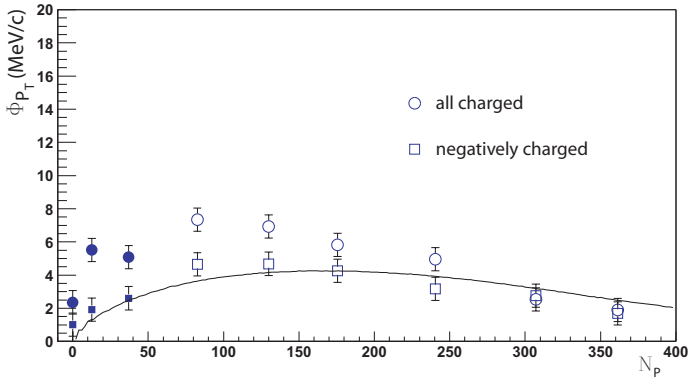

Figure 3: Φ_{P_T} versus the number of participants. Experimental data from NA49 Collaboration at SPS energies compared to our results(solid line).

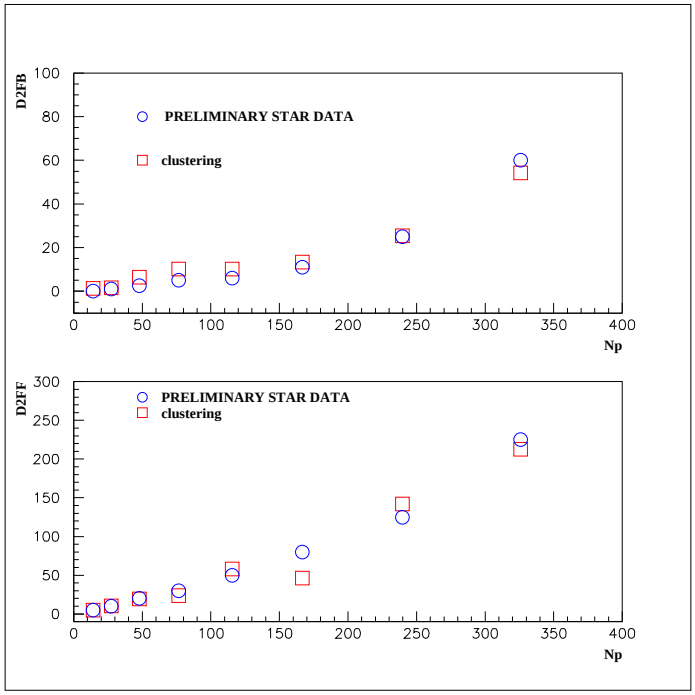

Figure 4: DFB^2 and DFF^2 versus the number of participants compared to PRELIMINARY STAR data

[4] M.M Aggarwal *et al.* [WA98 Collaboration], Phys. Rev. C **65**, 054912 (2002)

[5] K. Adox *et al.* [PHENIX Collaboration], Phys. Rev. C **66**, 024901 (2002).

[6] J. Adams *et al.* [STAR Collaboration] Phys. Rev. C **68**, 044905 (2003).

[7] J. T. Mitchell *et al.* [PHENIX Collaboration], this workshop.

[8] M. Gazdzicki *et al.* [NA49 Collaboration] J.Phys. G **30**, 5701 (2004).
M. Rybczynski *et al.* [NA49 Collaboration] J.Phys. Conf. Serv. **5**, 74 (2005).

[9] M. Rybczynski, this workshop.

[10] M. Lungwitz, this workshop.

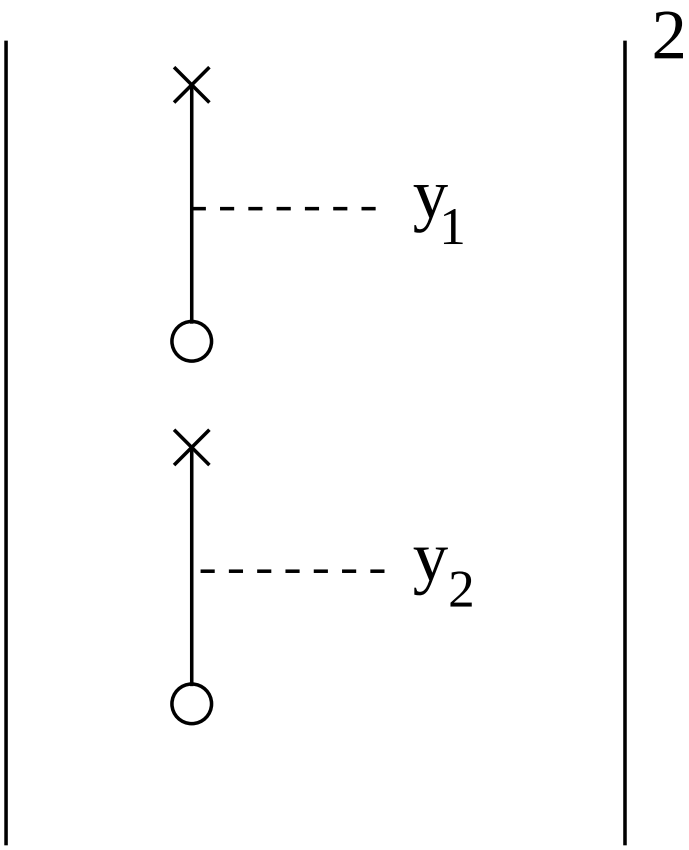

Figure 5: The leading order diagram which induce long range correlation in rapidity. The source of one nucleus is given by the x and that of the other by the O. The produced gluon is denoted by the dotted line.

[11] St. Mrowczynski, M. Rybczynski and Z. Wlodorczyk, Phys. Rev. C **70**, 054906 (2004).
G. Wilk and Z. Wlodorczyk Phys. Rev. Lett. **84**, 2770 (2000).

[12] N. Armesto, M. A. Braun, E. G. Ferreiro and C. Pajares, Phys. Rev. Lett **77**, 3736 (1996).

[13] E. G. Ferreiro, F. del Moral and C. Pajares, Phys. C **69**, 034901 (2004).

[14] L. Cunqueiro, E. G. Ferreiro, F. del Moral and C. Pajares, Phys. Rev. C **72**, 024907 (2005).

[15] A. Capella, U.P.Shukatme, C.I. Tan and Tran. Thanh. Van, Phys. Reports. 236,225 (1994).
A. Capella, C. Pajares and A. V. Ramallo, Nucl.Phys.B **241**, 75 (1984).

[16] N.Armesto, C.Pajares and D. Sousa, Phys. Lett. B **527**, 92 (2002).

[17] M. A. Braun and C. Pajares, Eur. Phys. J. C **16**, 349 (2000).
M. A. Braun and C. Pajares, Phys. Rev. Lett. **85**, 4864 (2001).

[18] J. Dias de Deus and C. Pajares, hep-ph/0607101.

[19] V. P. Konchakovski, S. Haussler, M. I. Gorenstein, E. L. Bratkovskaya, M. Bleicher and H. Stocker, Phys. Rev. C **73**, 034902 (2006).
M. Bleicher, this workshop

[20] S. S. Adler *et al.* [PHENIX Collaboration], Phys. Rev. Lett. **93**, 092301 (2004).

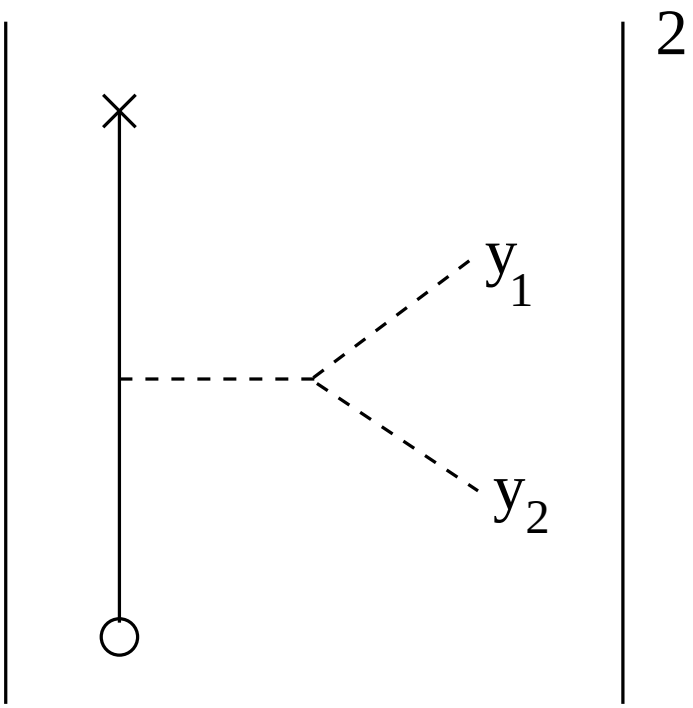

Figure 6: The leading order diagram which induce short range correlation in rapidity. Here two gluon from the different sources scatter and produce two gluons in the forward and backward hemisphere.

[21] J. Adams *et al.* J. Phys. G **32**, L37 (2006).

[22] T. Trainor, this workshop

[23] W. Broniowski, this workshop.
W. Broniowski, B. Hiller , W. Florkowski and P. Bozek, Phys. Lett. B **635**, 290 (2006).

[24] R. Blankenbecler, A. Capella, J. Tran Thanh Van, C. Pajares and A.V. Ramallo, Phys. Lett. B **107**, 106 (1981).
A. Kaidalov, Nucl. Phys. A **525**, 39 (1991).

[25] J. Dias de Deus, C. Pajares and C. A. Salgado, Phys. Lett. B **407**, 335 (1997).
J. Dias de Deus, C. Pajares and C. A. Salgado, Phys. Lett. B **409**, 474 (1997).
J. Dias de Deus, C. Pajares and C. A. Salgado, Phys. Lett. B **408**, 417 (1997).

[26] M. Faessler, Phys. Rep. **115**, 1 (1984).

[27] L. Cunqueiro, J. Dias de Deus and C. Pajares, Phys. Rev. C **74**, 034901 (2006).

[28] A. Capella and A. Krzywicki, Phys. Rev. D **18**, 4120 (1978).

[29] N. S. Amelin, N. Armesto, M. A. Braun, E.G. Ferreiro and C. Pajares, Phys. Rev. Lett **73**, 2813 (1994).

[30] M. A. Braun, R. S. Kolevatov, C. Pajares and V. V. Vechernin, Eur. Phys. J C **32**, 535 (2004).

[31] T. Tarnowsky [STAR Collaboration], nucl-ex/0606018.
S. Das, this workshop

[32] N. Armesto, L. Cunqueiro, E.G. Ferreiro and C. Pajares, to appear.

[33] N. Armesto, L. Maclerran and C. Pajares, hep-ph/0607345.